

# Correlation between mean transverse momentum and anisotropic flow in heavy-ion collisions

Giuliano Giacalone,<sup>1</sup> Fernando G. Gardim,<sup>2</sup> Jacquelyn Noronha-Hostler,<sup>3</sup> and Jean-Yves Ollitrault<sup>1</sup>

<sup>1</sup>*Université Paris Saclay, CNRS, CEA, Institut de physique théorique, 91191 Gif-sur-Yvette, France*

<sup>2</sup>*Instituto de Ciência e Tecnologia, Universidade Federal de Alfenas, 37715-400 Poços de Caldas, MG, Brazil*

<sup>3</sup>*Department of Physics, University of Illinois at Urbana-Champaign, Urbana, IL 61801, USA*

(Dated: January 17, 2022)

The correlation between the mean transverse momentum of outgoing particles,  $\langle p_t \rangle$ , and the magnitude of anisotropic flow,  $v_n$ , has recently been measured in Pb+Pb collisions at the CERN Large Hadron Collider, as a function of the collision centrality. We confirm the previous observation that event-by-event hydrodynamics predicts a correlation between  $v_n$  and  $\langle p_t \rangle$  that is similar to that measured in data. We show that the magnitude of this correlation can be directly predicted from the initial condition of the hydrodynamic calculation, for  $n = 2, 3$ , if one replaces  $v_n$  by the corresponding initial-state anisotropy,  $\varepsilon_n$ , and  $\langle p_t \rangle$  by the total energy per unit rapidity of the fluid at the beginning of the hydrodynamic expansion.

## I. INTRODUCTION

Anisotropic flow has been much studied in ultrarelativistic heavy-ion collisions, as it probes the properties of the little quark-gluon plasma formed in these collisions [1]. The event-by-event fluctuations of  $v_n$ , the  $n^{\text{th}}$  Fourier harmonic of the azimuthal distribution of the emitted hadrons, have been precisely characterized [2–4], as well as the mutual correlations between different flow harmonics [5–8]. Recently, following a suggestion by Božek [9], the ATLAS Collaboration has measured a correlation of a new type, namely, the correlation between the mean transverse momentum,  $\langle p_t \rangle$ , and  $v_n^2$  [10], a quantity dubbed  $\rho_n$ . Although event-by-event hydrodynamic results on  $\rho_n$  are in fair agreement with experimental data [11], a clear picture of the physical mechanism that produces this correlation is still missing.

In this paper, we explain the origin of the correlation between  $\langle p_t \rangle$  and  $v_n$  in hydrodynamic calculations. We first confirm, in Sec. II, that state-of-the-art hydrodynamic calculations yield results on  $\rho_n$  that are in agreement with recent Pb+Pb data. We use results from hydrodynamic calculations [12] obtained prior to the ATLAS analysis, so that they can be considered as predictions. We then unravel, in Sec. III, the physical mechanism behind  $\rho_n$ . While it is well established that  $v_2$  and  $v_3$  originate on an event-by-event basis from the anisotropies of the initial density profile,  $\varepsilon_n$  [13–18], the new crucial feature that we shall elucidate here is the origin of  $\langle p_t \rangle$  fluctuations in hydrodynamics. These fluctuations are thought to be driven by fluctuations in the fireball size,  $R$  [19, 20], a phenomenon referred to as size-flow transmutation [21]. We show in Sec. III A that, in fact, a much better predictor for  $\langle p_t \rangle$  is provided by the initial total energy per rapidity of the fluid [22]. On this basis, in Sec. III B we evaluate  $\rho_n$  using a standard initial-state model for Pb+Pb collisions, and we obtain results that are in good agreement with ATLAS data. We further show that agreement with data is instead lost if one uses  $R$  as an event-by-event predictor of  $\langle p_t \rangle$ .

## II. RESULTS FROM EVENT-BY-EVENT HYDRODYNAMICS

The ATLAS Collaboration measured the Pearson correlation coefficient between the mean transverse momentum and the anisotropic flow of the event [10]. Experimentally, this is obtained from a three-particle correlation introduced by Božek [9]. Since self correlations are subtracted in the measure of the correlation coefficient (i.e., one does not correlate a particle with itself), this observable is insensitive to trivial statistical fluctuations and probes genuine *dynamical* fluctuations [23], due to correlations. In hydrodynamics,  $\rho_n$  can be evaluated as:

$$\rho_n \equiv \frac{\langle \langle p_t \rangle v_n^2 \rangle - \langle \langle p_t \rangle \rangle \langle v_n^2 \rangle}{\sigma_{p_t} \sigma_{v_n^2}}, \quad (1)$$

where, following the notation of Ref.[20],  $\langle p_t \rangle$  denotes an average over the single-particle momentum distribution,  $f(p)$ , at freeze-out in a given event<sup>1</sup>, and the outer angular brackets denote an average over events in a given multiplicity (centrality) window.  $\sigma_{p_t}$  and  $\sigma_{v_n}$  denote, respectively, the standard deviation of  $\langle p_t \rangle$  and of  $v_n^2$ :

$$\begin{aligned} \sigma_{p_t} &\equiv \sqrt{\langle \langle p_t \rangle^2 \rangle - \langle \langle p_t \rangle \rangle^2}, \\ \sigma_{v_n^2} &\equiv \sqrt{\langle v_n^4 \rangle - \langle v_n^2 \rangle^2}. \end{aligned} \quad (2)$$

We evaluate  $\rho_n$  using hydrodynamic simulations. The setup of our calculation is the same as in Ref. [12]. We evolve 50000 minimum bias Pb+Pb collisions at  $\sqrt{s_{\text{NN}}} = 5.02$  TeV through the 2+1 viscous relativistic hydrodynamical code V-USPHYDRO [24–26]. The initial condition of the evolution is the profile of entropy density generated using the TRenTo model [27], tuned as in Ref. [28].<sup>2</sup>

<sup>1</sup> Using this notation, one can also write  $v_n \equiv |\langle e^{in\varphi} \rangle|$ , where  $\varphi$  is the azimuthal angle of the particle momentum.

<sup>2</sup> That is, we implement a geometric average of nuclear thickness

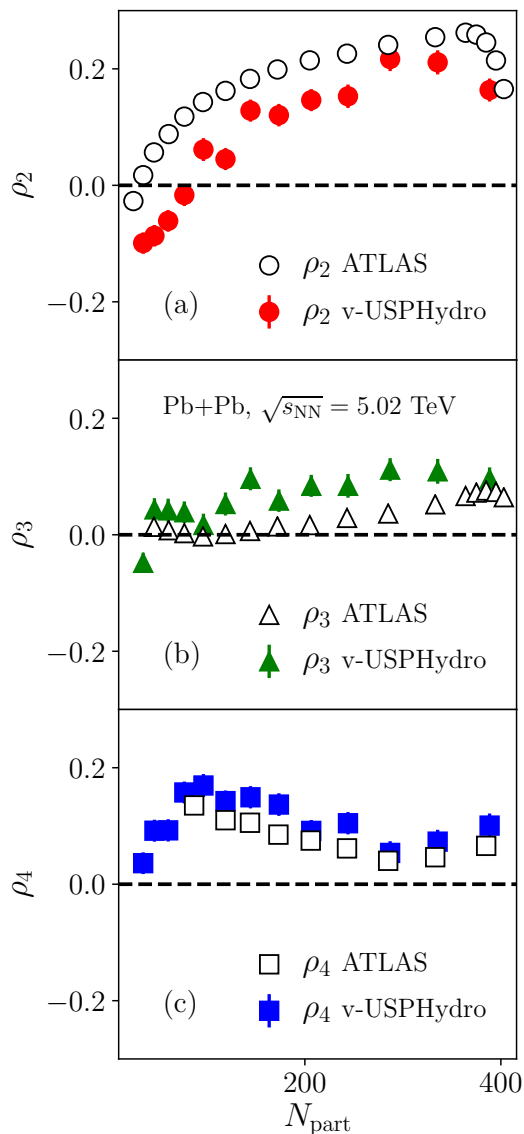


FIG. 1. (Color online) Value of  $\rho_n$  for  $n = 2$  (a),  $n = 3$  (b),  $n = 4$  (c), as a function of the number of participant nucleons in Pb+Pb collisions at  $\sqrt{s_{NN}} = 5.02$  TeV. Empty symbols are experimental results from the ATLAS Collaboration [10], while full symbols are hydrodynamic results [12].

We neglect the expansion of the system during the pre-equilibrium phase [29–31], and start hydrodynamics at time  $\tau_0 = 0.6$  fm/c after the collision [32]. We use the lattice QCD equation of state [33], and we implement a constant shear viscosity over entropy ratio  $\eta/s = 0.047$  [34].

functions (parameter  $p = 0$ ), where the thickness function of a nucleus is given by a linear superimposition of the thicknesses of the corresponding participant nucleons, modeled as Gaussian density profiles of width  $w = 0.51$  fm. The thickness of each participant nucleon is further allowed to fluctuate in normalization according to a gamma distribution of unit mean and standard deviation  $1/\sqrt{k}$ , with  $k = 1.6$ .

Fluid cells are transformed into hadrons [35] when the local temperature drops below 150 MeV. All hadronic resonances can be formed during this freeze-out process, and we implement subsequent strong decays into stable hadrons. To mimic the centrality selection performed in experiment, we sort events into centrality classes according to their initial entropy (5% classes are used). We evaluate hadron observables by integrating over the transverse momentum range  $0.2 < p_t < 3$  GeV/c, and over  $|\eta| < 0.8$ .<sup>3</sup>

In Fig. 1 we show our results along with ATLAS data. We choose data integrated over the  $0.5 < p_t < 2$  GeV/c, which is close to our setup. We conclude that event-by-event relativistic hydrodynamics captures semi-quantitatively the magnitude and the centrality dependence of  $\rho_2$ ,  $\rho_3$  and  $\rho_4$ .

### III. PHYSICAL ORIGIN OF $\rho_2$ AND $\rho_3$

#### A. Initial energy as a predictor for $\langle p_t \rangle$

The full hydrodynamic calculation allows us to reproduce the experimental data, but it does not give much insight into the physics underlying the observed  $\rho_n$ . In the same way as  $v_2$  and  $v_3$ , and their higher-order moments, are driven by the initial spatial eccentricity,  $\varepsilon_2$ , and triangularity,  $\varepsilon_3$ , on an event-by-event basis, it would be highly insightful to trace the origin of  $\rho_n$  back to the initial state of the hydrodynamic calculation. For this purpose, one must identify the property of the initial state which drives the event-by-event fluctuations of the mean transverse momentum.

It has recently been shown [22] that if one fixes the total entropy (which in an experiment amounts to fixing the centrality of the collision), then  $\langle p_t \rangle$  is essentially determined by the energy of the fluid per unit rapidity at the initial time  $\tau_0$ , which we denote by  $E_i$ :

$$E_i \equiv \tau_0 \int \epsilon(\tau_0, x, y) dx dy, \quad (3)$$

where  $\epsilon$  is the energy density, and the integral runs over the transverse plane. This is at variance with the earlier claims [19] that  $\langle p_t \rangle$  is determined by the initial transverse size of the fireball,  $R$ , defined as [20, 21]:

$$R^2 \equiv 2 \frac{\int (x^2 + y^2) s(\tau_0, x, y) dx dy}{\int s(\tau_0, x, y) dx dy} \quad (4)$$

where  $s$  is the entropy density.<sup>4</sup>

To illustrate the difference between these two predictors, we have evaluated  $E_i$ ,  $R$  and  $\langle p_t \rangle$  in event-by-event

<sup>3</sup> Note that the ATLAS detector has a wider acceptance in  $\eta$ , but this difference is unlikely to have any sizable effects on  $\rho_n$ .

<sup>4</sup> The factor 2 ensures that for a uniform entropy density  $s(\tau_0, x, y)$  in a circle of radius  $R$ , the right-hand side gives  $R^2$ .

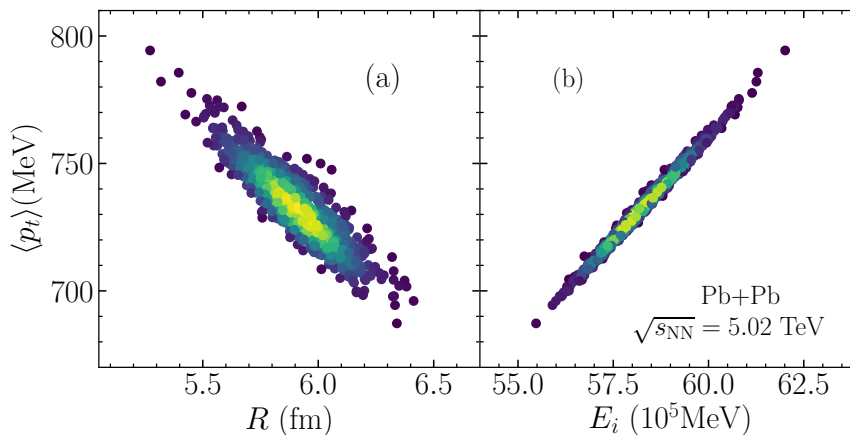


FIG. 2. (Color online) Results from ideal hydrodynamic simulations of Pb+Pb collisions at  $\sqrt{s_{NN}} = 5.02$  TeV at impact parameter  $b = 2.5$  fm. 850 events have been simulated, where each event has the same total entropy, but a different entropy density profile. Each symbol represents a different event. (a) Scatter plot of the mean transverse momentum of charged particles,  $\langle p_t \rangle$ , versus the initial size,  $R$ , defined by Eq. (4). (b) Scatter plot of  $\langle p_t \rangle$  versus the initial energy per unit rapidity,  $E_i$ , defined by Eq. (3).

hydrodynamics at fixed initial entropy. Note that the minimum bias calculation performed in Sec. II is not well-suited for this purpose, as, even if we narrowed down the width of our centrality bins by a factor 2, there would still be significant entropy fluctuations in our sample. For this reason, we resort to the calculation shown in Ref. [22]. Here the events are evaluated at fixed impact parameter  $b = 2.5$  fm, and at fixed total entropy corresponding to the mean entropy of Pb+Pb collisions at  $\sqrt{s_{NN}} = 5.02$  TeV in the 0-5% centrality window. Also, we perform an ideal hydrodynamic expansion, which ensures conservation of entropy. The initial condition of the calculation, the equation of state, and the initialization time,  $\tau_0$ , are the same used in the calculation of Sec. II.<sup>5</sup> This calculation is evolved through the MUSIC hydrodynamic code [37–39].

Figure 2(a) displays the scatter plot of  $R$  vs.  $\langle p_t \rangle$  obtained in this calculation. These two quantities are negatively correlated, as already shown by other authors [21]. The explanation is that for a fixed total entropy, a smaller size generally implies a larger entropy density, hence a larger temperature, which in turn implies a larger  $\langle p_t \rangle$  [40]. There is, however, a significant spread of the values of  $\langle p_t \rangle$  for a fixed  $R$ . By contrast, there is an almost one-to-one correspondence between  $\langle p_t \rangle$  and the initial energy,  $E_i$ , as displayed in Fig. 2 (b). We shall show now that, in order to understand the measured correlation between  $\langle p_t \rangle$  and  $v_n$ , it is indeed crucial to employ  $E_i$  as a predictor of the average transverse momentum.

## B. Results from models of initial conditions

We first explain how  $\rho_n$ , defined in Eq. (1), can be evaluated from the initial conditions of the hydrodynamic calculations. First, one uses the approximate proportionality between  $v_n$  and the initial anisotropy  $\varepsilon_n$  [17] for  $n = 2, 3$ :

$$v_n = \kappa_n \varepsilon_n, \quad (5)$$

where  $\kappa_n$  is a response coefficient which is the same for all events at a given centrality.<sup>6</sup> Next, one uses the observation, made in Sec. III A, that  $\langle p_t \rangle = f(E_i)$ , where  $f(E_i)$  is some smooth function of the initial energy,  $E_i$ . Linearizing in the fluctuations of  $E_i$  and  $\langle p_t \rangle$  around their mean values,  $\langle E_i \rangle$  and  $\langle \langle p_t \rangle \rangle$ , one obtains

$$\langle p_t \rangle - \langle \langle p_t \rangle \rangle = f'(\langle E_i \rangle) (E_i - \langle E_i \rangle). \quad (6)$$

Inserting Eqs. (5) and (6) into Eq. (1), one obtains:

$$\rho_n = \frac{\langle E_i \varepsilon_n^2 \rangle - \langle E_i \rangle \langle \varepsilon_n^2 \rangle}{\sigma_{E_i} \sigma_{\varepsilon_n^2}} \frac{f'(\langle E_i \rangle)}{|f'(\langle E_i \rangle)|}, \quad (7)$$

where  $\sigma_{E_i}$  and  $\sigma_{\varepsilon_n^2}$  denote the standard deviations, obtained by replacing  $\langle p_t \rangle$  and  $v_n$  with  $E_i$  and  $\varepsilon_n$  in Eq. (2). Remarkably enough, the dependence on the unknown function  $f(E_i)$  cancels, except for the sign of  $f'(\langle E_i \rangle)$ .

An important advantage of Eq. (7) is that it allows us to evaluate  $\rho_n$  in millions of simulated initial conditions with little computational effort, and thus to overcome the

<sup>5</sup> The sole differences are that we implement slightly smaller entropy fluctuations, using  $k = 2$  in TRIENTO, which provide a better fit of LHC data [12], as well as a slightly higher freeze-out temperature  $T_f = 156.5$  MeV, which has now become a more standard choice [36].

<sup>6</sup> This linear response works for  $v_2$  and  $v_3$ , but not for  $v_4$  [16], so that we do not discuss  $\rho_4$  in this section.

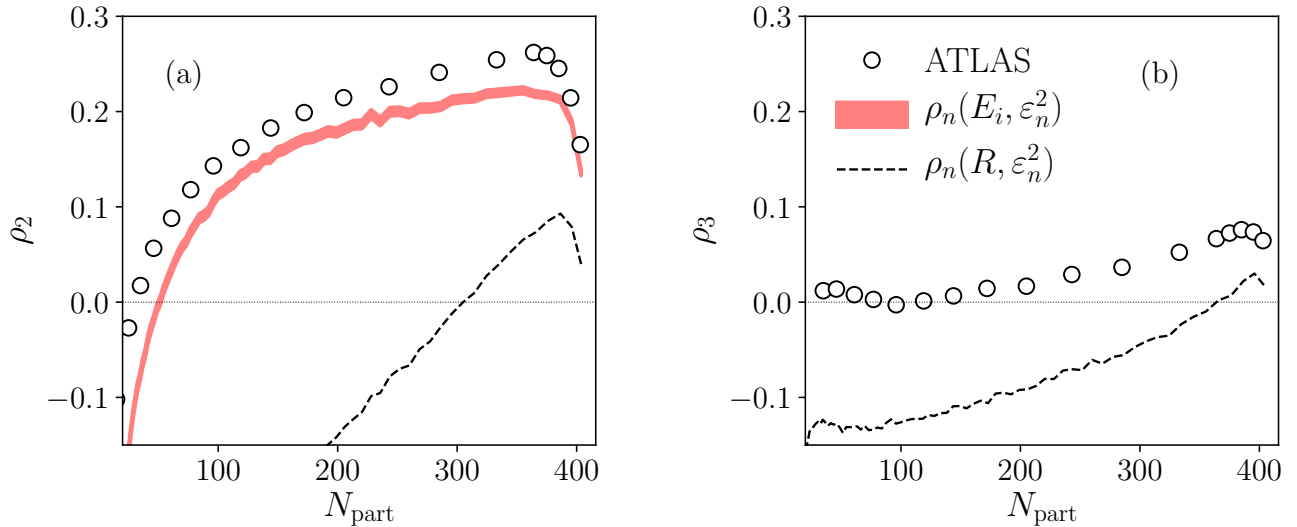


FIG. 3. (Color online) Variation of  $\rho_2$  (a) and  $\rho_3$  (b) with the number of participants in Pb+Pb collisions at  $\sqrt{s_{\text{NN}}} = 5.02$  TeV. As in Fig. 1, symbols are experimental results from the ATLAS Collaboration [10]. The shaded band is our result using Eq. (7). The width of the band is the statistical error evaluated through jackknife resampling. The dashed line is obtained by replacing  $E_i$  with  $R$  in Eq. (7).

issue of large entropy fluctuations within a finite centrality bin [11]. This allows us, hence, to evaluate  $\rho_n$  in the strict limit of fixed initial entropy, and to reproduce the situation of Fig. 2 in a minimum bias calculation.

To this aim we have generated 20 million minimum bias Pb+Pb events using the same T<sub>R</sub>ENTo parametrization as in Fig. 2. We sort the events into narrow 0.25% centrality bins, and in each bin we evaluate  $\rho_n$  according to Eq. (7). To evaluate  $E_i$  in each event, we assume that the entropy profile returned by T<sub>R</sub>ENTo,  $s$ , is related to the energy density,  $\epsilon$ , of the event through  $\epsilon \propto s^{4/3}$ . This is typically a very good approximation at the high temperatures achieved in the initial state of nucleus-nucleus collisions. Our result is displayed in Fig. 3 as a shaded band. Note that we recombine 0.25% bins into 1% bins for sake of visualization. Our T<sub>R</sub>ENTo calculation is in good agreement with ATLAS data (open symbols) for both  $\rho_2$  and  $\rho_3$ , and is consistent with the full hydrodynamic calculation shown in Fig. 1, in the sense that both evaluations slightly underestimates  $\rho_2$  while they overestimates  $\rho_3$ . Note that  $\rho_2$  and  $\rho_3$  measured by the ATLAS Collaboration have a slight dependence on the  $p_t$  cut used in the analysis [10]. The difference between our results and experimental data is of the same order, or smaller, than the dependence of experimental results on the  $p_t$  cuts. This feature is not captured by our prediction, which is independent of these cuts by construction. It would be therefore interesting to have new measurements of  $\rho_n$  with a lower  $p_t$  cut, of order 0.2 or 0.3 GeV, which is where the bulk of the produced particles sits. This may improve agreement between our evaluations and data.

While the quantitative results shown in Fig. 3 depend on the parametrization of the T<sub>R</sub>ENTo model, we

show in Appendix A that the main qualitative features, for instance the fact that  $\rho_n$  is positive in central collisions, are robust and model-independent. It is interesting though that the choice of parameters made here, namely,  $p = 0$ , preferred from previous comparisons [18, 28], and  $k = 2$  [12], also optimizes agreement with  $\rho_n$  data. We have also checked that the stringent condition of having a fixed total entropy,  $S$ , can be relaxed by replacing  $E_i$  with  $E_i/S$  in Eq. (7). With this choice, results are essentially unchanged if one uses 2% centrality bins. A moderate variation starts to be visible if one uses 5% bins, as with other observables [41].

Finally, we show how the results are changed if one uses the initial size,  $R$ , as a predictor of  $\langle p_t \rangle$ . If one replaces  $E_i$  with  $R$  in Eq. (7), the resulting value of  $\rho_n$  is completely different, as shown by the dashed lines in Fig. 3.<sup>7</sup> These results show that, at fixed centrality, the correlation between  $\langle p_t \rangle$  and  $v_n^2$  is *not* driven by the event-by-event fluctuations of the fireball size. Note however that a better geometric predictor can be constructed following Schenke, Shen and Teaney [42], whose paper appeared while we were finalizing this manuscript. They show that if one replaces the rms size,  $R$ , with the area of the elliptical region of nuclear overlap,  $R^2 \sqrt{1 - \varepsilon_2^2}$ , then the quality of the predictor for  $\rho_2$  improves greatly.

<sup>7</sup> Note that the correlation between  $R$  and  $\langle p_t \rangle$  is negative, as shown in Fig. 2 (a). This implies  $f'(\langle R \rangle) < 0$  in the right-hand side of Eq. (7), resulting in an overall negative sign.

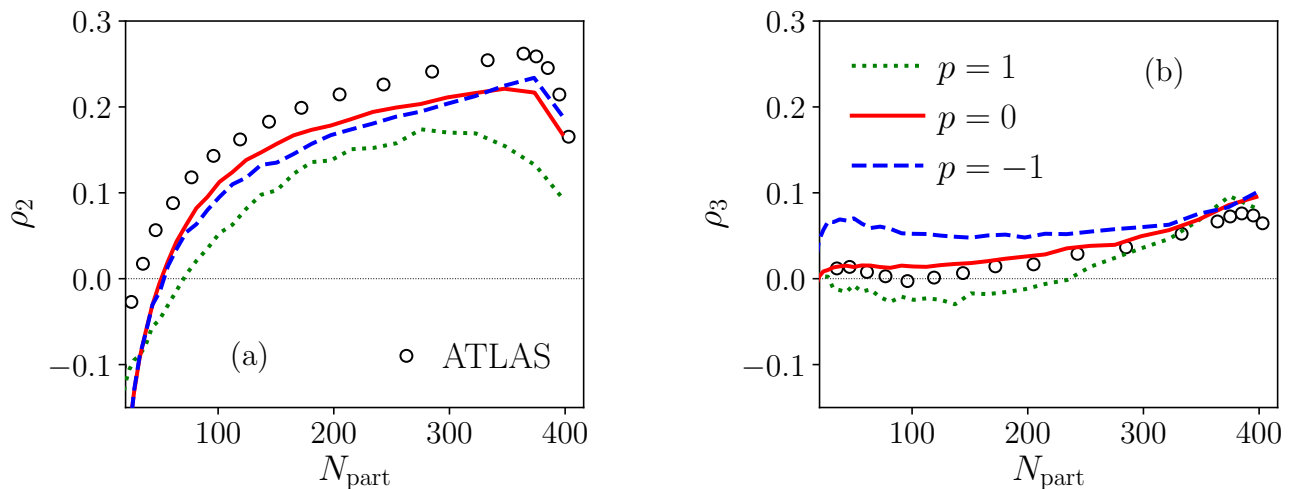


FIG. 4. (Color online) Dependence of  $\rho_2$  (a) and  $\rho_3$  (b) on the parameter  $p$  in the TReNTo model. Full lines:  $p = 0$  (entropy density  $s \propto \sqrt{T_A T_B}$ ), as in Fig. 3. Dotted lines:  $p = 1$  ( $s \propto T_A + T_B$ ). Dashed lines:  $p = -1$  ( $s \propto T_A T_B / (T_A + T_B)$ ). We use broader centrality bins for this calculation than for Fig. 3, which explains the small differences between the  $p = 0$  results of the two figures. As in Figs. 1 and 3, symbols are ATLAS data [10].

#### IV. CONCLUSIONS

We have shown that ATLAS results on  $\rho_n$  in Pb+Pb collisions can be explained by hydrodynamics. The mechanism driving the correlation between the mean transverse momentum and anisotropic flow in Pb+Pb collisions can be traced back to the initial density profile, i.e., to the early stages of the collision. This implies in turn that this observable has limited sensitivity to the details of the hydrodynamic expansion in general, and to the transport coefficients of the fluid in particular, as nicely confirmed by the hydrodynamic results (Fig. 9) of Ref. [42]. We have found that  $\langle p_t \rangle$  fluctuations are driven by fluctuations of the initial energy over entropy ratio  $E_i/S$ , and not by the fluctuations of the fireball size as previously thought. By use of Eq. (7), models of initial conditions that fit anisotropic flow data and multiplicity fluctuations also naturally reproduce the centrality dependence of  $\rho_2$  and  $\rho_3$  measured by the ATLAS Collaboration without any further adjustment. Note that experimental data are also available for p+Pb collisions, the study of which we leave for future work.

#### ACKNOWLEDGMENTS

FGG was supported by CNPq (Conselho Nacional de Desenvolvimento Científico) grant 312932/2018-9, by INCT-FNA grant 464898/2014-5 and FAPESP grant 2018/24720-6. G.G., M.L. and J.-Y.O. were supported by USP-COFECUB (grant Uc Ph 160-16, 2015/13). J.N.H.

acknowledges the support of the Alfred P. Sloan Foundation, support from the US-DOE Nuclear Science Grant No. de-sc0019175. J.-Y. O. thanks Piotr Bożek for discussions. G.G. acknowledges useful discussions with Derek Teaney and Björn Schenke.

#### Appendix A: Varying the parametrization of the initial profile

We check the sensitivity of  $\rho_n$ , as defined by Eq. (7), to the parametrization of initial conditions. Figure 4 displays the variation of  $\rho_n$  for three different values of  $p$  in the TReNTo model. Several qualitative trends are robust:  $\rho_2$  and  $\rho_3$  are both positive for central collisions; As the number of participants decreases from its maximum value,  $\rho_2$  steeply increases and then decreases, eventually becoming negative, while the centrality dependence of  $\rho_3$  is milder. But significant differences appear at the quantitative level, and the value  $p = 0$ , which is the preferred value also for other observables [18, 28], agrees best with the recent  $\rho_n$  data. We have also studied the dependence on the parameter  $k$  governing the magnitude of fluctuations in TReNTo. Results in Fig. 3 are obtained with  $k = 2$ , but we have also carried out calculations with  $k = 1$ , corresponding to larger fluctuations. We have found (not shown) that the results for  $\rho_2$  are essentially unchanged except for a minor increase in central collisions, while the variation of  $\rho_3$  becomes flatter, similar to the  $p = -1$  results in Fig. 4.

- [2] G. Aad *et al.* [ATLAS Collaboration], JHEP **1311**, 183 (2013) doi:10.1007/JHEP11(2013)183 [arXiv:1305.2942 [hep-ex]].
- [3] A. M. Sirunyan *et al.* [CMS Collaboration], Phys. Lett. B **789**, 643 (2019) doi:10.1016/j.physletb.2018.11.063 [arXiv:1711.05594 [nucl-ex]].
- [4] S. Acharya *et al.* [ALICE Collaboration], Phys. Rev. Lett. **123**, no. 14, 142301 (2019) doi:10.1103/PhysRevLett.123.142301 [arXiv:1903.01790 [nucl-ex]].
- [5] G. Aad *et al.* [ATLAS Collaboration], Phys. Rev. C **90**, no. 2, 024905 (2014) doi:10.1103/PhysRevC.90.024905 [arXiv:1403.0489 [hep-ex]].
- [6] J. Adam *et al.* [ALICE Collaboration], Phys. Rev. Lett. **117**, 182301 (2016) doi:10.1103/PhysRevLett.117.182301 [arXiv:1604.07663 [nucl-ex]].
- [7] A. M. Sirunyan *et al.* [CMS Collaboration], arXiv:1910.08789 [hep-ex].
- [8] S. Acharya *et al.* [ALICE Collaboration], arXiv:2002.00633 [nucl-ex].
- [9] P. Bozek, Phys. Rev. C **93**, no. 4, 044908 (2016) doi:10.1103/PhysRevC.93.044908 [arXiv:1601.04513 [nucl-th]].
- [10] G. Aad *et al.* [ATLAS Collaboration], Eur. Phys. J. C **79**, no. 12, 985 (2019) doi:10.1140/epjc/s10052-019-7489-6 [arXiv:1907.05176 [nucl-ex]].
- [11] P. Bozek and H. Mehrabpour, arXiv:2002.08832 [nucl-th].
- [12] G. Giacalone, J. Noronha-Hostler, M. Luzum and J. Y. Ollitrault, Phys. Rev. C **97**, no. 3, 034904 (2018) doi:10.1103/PhysRevC.97.034904 [arXiv:1711.08499 [nucl-th]].
- [13] B. Alver *et al.* [PHOBOS Collaboration], Phys. Rev. Lett. **98**, 242302 (2007) doi:10.1103/PhysRevLett.98.242302 [nucl-ex/0610037].
- [14] B. Alver and G. Roland, Phys. Rev. C **81**, 054905 (2010) Erratum: [Phys. Rev. C **82**, 039903 (2010)] doi:10.1103/PhysRevC.82.039903, 10.1103/PhysRevC.81.054905 [arXiv:1003.0194 [nucl-th]].
- [15] D. Teaney and L. Yan, Phys. Rev. C **83**, 064904 (2011) doi:10.1103/PhysRevC.83.064904 [arXiv:1010.1876 [nucl-th]].
- [16] F. G. Gardim, F. Grassi, M. Luzum and J. Y. Ollitrault, Phys. Rev. C **85**, 024908 (2012) doi:10.1103/PhysRevC.85.024908 [arXiv:1111.6538 [nucl-th]].
- [17] H. Niemi, G. S. Denicol, H. Holopainen and P. Huovinen, Phys. Rev. C **87**, no. 5, 054901 (2013) doi:10.1103/PhysRevC.87.054901 [arXiv:1212.1008 [nucl-th]].
- [18] G. Giacalone, J. Noronha-Hostler and J. Y. Ollitrault, Phys. Rev. C **95**, no. 5, 054910 (2017) doi:10.1103/PhysRevC.95.054910 [arXiv:1702.01730 [nucl-th]].
- [19] W. Broniowski, M. Chojnacki and L. Obara, Phys. Rev. C **80**, 051902 (2009) doi:10.1103/PhysRevC.80.051902 [arXiv:0907.3216 [nucl-th]].
- [20] P. Bozek and W. Broniowski, Phys. Rev. C **85**, 044910 (2012) doi:10.1103/PhysRevC.85.044910 [arXiv:1203.1810 [nucl-th]].
- [21] P. Boek and W. Broniowski, Phys. Rev. C **96**, no. 1, 014904 (2017) doi:10.1103/PhysRevC.96.014904 [arXiv:1701.09105 [nucl-th]].
- [22] F. G. Gardim, G. Giacalone, M. Luzum and J. Y. Ollitrault, arXiv:2002.07008 [nucl-th].
- [23] J. Adams *et al.* [STAR Collaboration], Phys. Rev. C **72**, 044902 (2005) doi:10.1103/PhysRevC.72.044902 [nucl-ex/0504031].
- [24] J. Noronha-Hostler, G. S. Denicol, J. Noronha, R. P. G. Andrade and F. Grassi, Phys. Rev. C **88**, no. 4, 044916 (2013) doi:10.1103/PhysRevC.88.044916 [arXiv:1305.1981 [nucl-th]].
- [25] J. Noronha-Hostler, J. Noronha and F. Grassi, Phys. Rev. C **90**, no. 3, 034907 (2014) doi:10.1103/PhysRevC.90.034907 [arXiv:1406.3333 [nucl-th]].
- [26] J. Noronha-Hostler, J. Noronha and M. Gyulassy, Phys. Rev. C **93**, no. 2, 024909 (2016) doi:10.1103/PhysRevC.93.024909 [arXiv:1508.02455 [nucl-th]].
- [27] J. S. Moreland, J. E. Bernhard and S. A. Bass, Phys. Rev. C **92**, no. 1, 011901 (2015) doi:10.1103/PhysRevC.92.011901 [arXiv:1412.4708 [nucl-th]].
- [28] J. E. Bernhard, J. S. Moreland, S. A. Bass, J. Liu and U. Heinz, Phys. Rev. C **94**, no. 2, 024907 (2016) doi:10.1103/PhysRevC.94.024907 [arXiv:1605.03954 [nucl-th]].
- [29] J. Vredevoogd and S. Pratt, Phys. Rev. C **79**, 044915 (2009) doi:10.1103/PhysRevC.79.044915 [arXiv:0810.4325 [nucl-th]].
- [30] W. van der Schee, P. Romatschke and S. Pratt, Phys. Rev. Lett. **111**, no. 22, 222302 (2013) doi:10.1103/PhysRevLett.111.222302 [arXiv:1307.2539 [nucl-th]].
- [31] A. Kurkela, A. Mazeliauskas, J. F. Paquet, S. Schlichting and D. Teaney, Phys. Rev. Lett. **122**, no. 12, 122302 (2019) doi:10.1103/PhysRevLett.122.122302 [arXiv:1805.01604 [hep-ph]].
- [32] P. F. Kolb, P. Huovinen, U. W. Heinz and H. Heiselberg, Phys. Lett. B **500**, 232 (2001) doi:10.1016/S0370-2693(01)00079-X [hep-ph/0012137].
- [33] S. Borsanyi, Z. Fodor, C. Hoelbling, S. D. Katz, S. Krieg and K. K. Szabo, Phys. Lett. B **730**, 99 (2014) doi:10.1016/j.physletb.2014.01.007 [arXiv:1309.5258 [hep-lat]].
- [34] P. Alba, V. Mantovani Sarti, J. Noronha, J. Noronha-Hostler, P. Parotto, I. Portillo Vazquez and C. Ratti, Phys. Rev. C **98**, no. 3, 034909 (2018) doi:10.1103/PhysRevC.98.034909 [arXiv:1711.05207 [nucl-th]].
- [35] D. Teaney, Phys. Rev. C **68**, 034913 (2003) doi:10.1103/PhysRevC.68.034913 [nucl-th/0301099].
- [36] A. Bazavov *et al.* [HotQCD Collaboration], Phys. Lett. B **795**, 15 (2019) doi:10.1016/j.physletb.2019.05.013 [arXiv:1812.08235 [hep-lat]].
- [37] B. Schenke, S. Jeon and C. Gale, Phys. Rev. C **82**, 014903 (2010) doi:10.1103/PhysRevC.82.014903 [arXiv:1004.1408 [hep-ph]].
- [38] B. Schenke, S. Jeon and C. Gale, Phys. Rev. Lett. **106**, 042301 (2011) doi:10.1103/PhysRevLett.106.042301 [arXiv:1009.3244 [hep-ph]].
- [39] J. F. Paquet, C. Shen, G. S. Denicol, M. Luzum, B. Schenke, S. Jeon and C. Gale, Phys. Rev. C **93**, no. 4, 044906 (2016) doi:10.1103/PhysRevC.93.044906 [arXiv:1509.06738 [hep-ph]].
- [40] F. G. Gardim, G. Giacalone, M. Luzum and J. Y. Ollitrault, arXiv:1908.09728 [nucl-th].

- [41] F. G. Gardim, F. Grassi, M. Luzum and J. Noronha-Hostler, Phys. Rev. C **95**, no. 3, 034901 (2017) doi:10.1103/PhysRevC.95.034901 [arXiv:1608.02982 [nucl-th]].
- [42] B. Schenke, C. Shen and D. Teaney, [arXiv:2004.00690 [nucl-th]].